Journal of GeoEngineering, Vol. 10, No. 2, pp. 35-43, August 2015
http://dx.doi.org/10.6310/jog.2015.10(2).1

NUMERICAL SIMULATION OF ROCK CUTTING IN DIFFERENT CUTTING MODE USING THE DISCRETE ELEMENT METHOD

Qian-Qian Zhang[1], Zhen-Nan Han[2*], Shao-Hui Ning[3], Qiu-Zu Liu[4], and Rui-Wu Guo[5]

ABSTRACT

The paper presents numerical modeling of rock cutting tests by using the discrete element method (DEM). The particle assemblies were generated by the specimen-genesis procedure, representing Medium-grade chromite and three types of sandstone. The solid models of pick with rounded tip built by Pro/ENGINEER5.0 were imported into Particle Flow Code in 3 Dimensions (PFC^{3D}), then the models of rock cutting were established. The macro-properties of the particle assemblies were calibrated by modeling the unconfined compressive strength and Brazilian tests. The particle assemblies were cut by pick at a constant velocity in unrelieved and relieved cutting modes, the crack propagation was observed, and the forces acting on pick were monitored. The mean peak cutting forces in unrelieved cutting mode, the mean forces in relieved cutting mode and the ratio of peak to mean forces in both cutting mode obtained from numerical and experimental studies were compared respectively. It was concluded that the mean forces, mean peak forces and the ratio of peak to mean forces were predicted accurately in the numerical simulation. In addition, according to the analysis of the variations of forces with cutting distance, the mean cutting force and the mean normal force obtained in relieved cutting mode are lower than those in unrelieved mode, and an important conclusion can be drawn that the influence of the adjacent cut plays a substantial part during the cutting process. Furthermore, the figures showed that the number of cracks in tensile failure is about three times as large as in shear failure in this simulation, thus the fractures formed in the condition of tensile failure as the main failure mode. Based on this study, it is determined that DEM is a suitable method to carry out the simulation of rock cutting test and to observe the crack propagation.

Key words: Discrete element method, solid models, unrelieved cutting, relieved cutting, mean force, tensile failure.

1. INTRODUCTION

During the rock cutting process, the forces acting on picks have been influenced the pick's life and stability in directly. Prediction of the forces was significant to the selection and design of picks and cutterhead. Many researchers did a lot of theoretical, experimental and numerical studies about the rock cutting process. The theoretical model proposed by Evans (1984) and the later correction models of Evans' theory proposed by Goktan (1997) and Roxborough and Liu (1995) respectively have been widely used in rock cutting with the chisel-shaped and pointed attack picks. However, influenced by some factors in the poor working conditions, there is a big gap between the theoretical and experimental results. The pick forces can be measured reliably by experiment, but the experimental process will waste plenty of time and costs high. With the development of computer technology, the numerical simulation has become more mature and widely used. Discrete Element Method (DEM) has a wide application in rock mechanics, soil mechanics, structural analysis, granular materials, material processing, fluid mechanics, *etc*. It has the great advantage to create the particle assembly which can be reflects the physical properties of rock.

An overview of the discrete element simulation of rock cutting was briefly described as follows: The first trial of the numerical simulation of rock cutting utilizing PFC^{3D} was accomplished by Su and Akcin (2008), then the larger rock specimen was established, and the depth of cut of 3 mm was selected in rock-tool model (Su and Akcin 2009). In order to validate the feasibility of PFC^{3D} in simulation of rock cutting test, graded particle assembly consisted of four areas in the shape of half cylinders was established, and the numerical results with those obtained from theoretical and experimental studies were compared (Su 2011). Rojek and Onate (2011) presented the DEM models of rock cutting processes (both 2D and 3D models) to study the rock fracturing. Moon and Oh (2012) proposed a multi-indentation model by using DEM to study the optimum rock cutting conditions. More recently, a rock-tool model took tribological interactions into account was established, and the numerical simulations were carried out by different tools, and the results show that the depth of cut and pick wear have a great influence on pick forces in the cutting process (Van Wyk *et al*. 2014).

In this study, the models of rock cutting tests were established depending on the principle of discrete element method, and simulated in unrelieved and relieved cutting modes by using the pick with rounded tip. The numerical results and those obtained from theoretical and experimental studies in

Manuscript received February 4, 2015; revised May 25, 2015; accepted June 9, 2015.
[1] Ph.D. student, School of Mechanical Engineering, Taiyuan University of Technology, Taiyuan, Shanxi, 030024, China.
[2] Professor (corresponding author), School of Mechanical Engineering, Taiyuan University of Technology, Taiyuan, Shanxi, 030024, China (e-mail: ginatyut@163.com).
[3] Ph.D. student, School of Mechanical Engineering, Taiyuan University of Science and Technology, Taiyuan, Shanxi, 030024, China.
[4] Ph.D. student, School of Mechanical Engineering, Taiyuan University of Technology, Taiyuan, Shanxi, 030024, China.
[5] Master student, School of Mechanical Engineering, Taiyuan University of Technology, Taiyuan, Shanxi, 030024, China.

both cutting modes were compared and discussed in detail. The relationships between the number of cracks in tensile failure and those obtained in shear failure was also examined and the main failure mode was determined.

2. PREDICTION OF THE CUTTING FORCES

Prediction of the mean peak cutting force acting on pick have been investigated from the theoretical, experimental and numerical models, and some widely used theories were supported by the results obtained from laboratory. However, the theoretical models of mean peak cutting force only apply to the unrelieved cutting mode, while the numerical simulation has the advantage of implement easily and varying the cutting parameters freely, it has been became a widely accepted method in rock cutting.

2.1 Rock Cutting Mode

The rock cutting tests can be conducted at two different types: Unrelieved and relieved cutting mode. In relieved cutting mode, as is shown in Fig. 1(a), microcracks formed in adjacent cuts can be effectively connection, the debris were detached from the rock mass under the condition of shear failure as the main failure mode, and having uniform size characteristics. In unrelieved cutting mode, as is shown in Fig. 1(b), since the cutter spacing is larger, microcracks formed in current cut can't be effectively growth and extended to those formed in previous cut, the debris were detached in the condition of compression failure as the main failure mode, and the chunk of debris can't be formed, resulting in the energy consumption is higher than that in relieved cutting mode. The cutter spacing is not too large or too small. If it is too large, a big ridge between the adjacent cuts will be formed and it couldn't reflect the beneficial effects of interaction between the picks. If it is too small, a considerable overcutting or grinding will occur and large amount of dust will be prone to generate. It is known that the optimum ratio of spacing to the cut of depth is found to be a reasonably constant in a given rock.

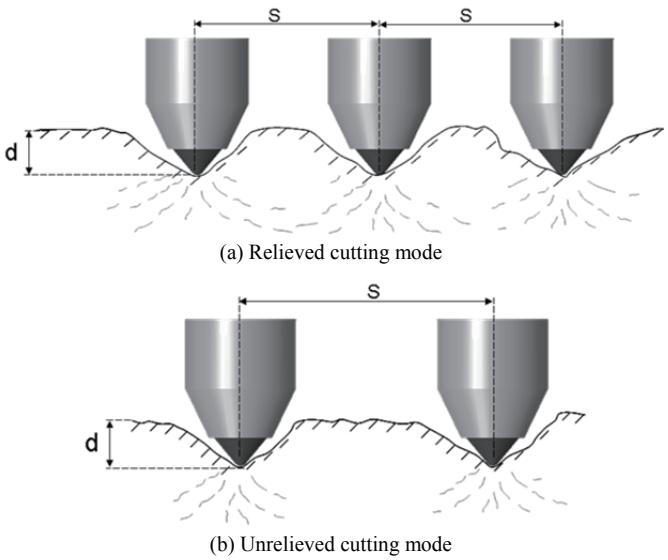

Fig. 1 Effect of cutter spacing on rock cutting

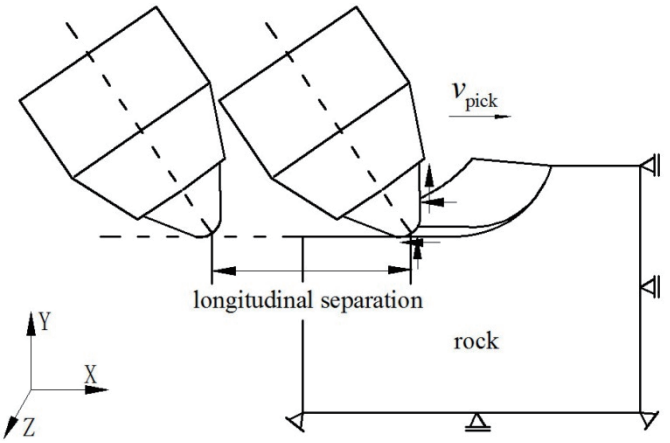

Fig. 2 Geometrical scheme of a rock cutting model

2.2 Numerical Model of the Rock Cutting

The paper presents a rock cutting model in both unrelieved and relieved cutting modes, and it consists of rock specimen and two picks with rounded tip which arranged in a given spacing (Fig. 2). The specimen was composed of massive spherical particles and cemented by the bond elements. In order to reflect the physical and mechanical properties of rocks, particle size should have to be much smaller and this would make computations more time-consuming. Therefore, a suitable range of particle size was selected by comprehensive considering the running time of programs and the depth of cut, we aimed to make it sure that the pick would be interacting with minimum three particles in rock specimen.

The previous researchers were studied the rock cutting in PFC^{2D} or PFC^{3D} by using the pick with sharp tip, but the actual pick tip was rounded. Moreover, the geometric characteristics of pick have a very large influence on the forces acting on it (Yong *et al*. 2010). After the pick was installed, the contact area and direction between pick and rock were determined by the geometry of tip including shape and radius. In order to be consistent with the test conditions, the actual measured size of pick was used in this study. We choose the first 1/3 of the extended portion of pick to simplify pick model, that is to say, remove the pick body which can't contact the particles in the cutting process to improve the computational efficiency. The solid models of the simplified pick were built by Pro/ENGINEER5.0 whose geometry of tip are the same to S-35/80 H conical pick manufactured by Sandvik, and the corresponding STL format file was exported, then the data of solid models was imported into PFC^{3D} through the Fish file: CAD-support.FIS, and the pick was regarded as rigid body.

2.3 Theoretical and Experimental Models

Many researchers have been done a lot of studies on the theoretical aspect of rock cutting, and the mathematical models of mean peak cutting force acting on pick were established.

Evans first presented the theoretical model which described the cutting mechanism of coal, and its extended theory was widely used in the design of shearer, boring machines and other mining equipments. It was proved that the tensile strength and compressive strength were the dominant rock properties affecting the performance of conical pick during the rock cutting. Theoretical formula is (Evans 1984):

$$FC' = \frac{16\pi\sigma_t^2 d^2}{\cos^2(\phi/2)\,\sigma_c} \quad (1)$$

where FC' is the peak cutting force, d is the depth of cut, ϕ is the tip angle, σ_t is the tensile strength, σ_c is the uniaxial compressive strength.

Later, Roxborough and Liu (1995) amended the Evans' theory for point attack tools by introducing the friction angle between cutting tool and rock.

$$FC' = \frac{16\pi\,\sigma_c\, d^2\sigma_t^2}{\left(2\sigma_t + \left(\sigma_c\cos(\phi/2)/\left[(1+\tan\gamma)/\tan(\phi/2)\right]\right)\right)^2} \quad (2)$$

where γ is the friction angle between the tool and rock, which is assumed to be between 16° and 30°, other notations are as given in Eq. (1).

The theoretical model proposed by Goktan overcame some shortcomings of Evans' theory, such as when the half-angle of pick was 0, cutting force could not be reduced to 0, and the friction angle between the tool and rock was not considered, *etc*. The compressive strength was removed from the formula, which made it more convenient to calculate the mean peak cutting force. The formula is as follows (Gokan 1997):

$$FC' = \frac{4\pi\sigma_t\, d^2 \sin^2(\phi/2+\gamma)}{\cos(\phi/2+\gamma)} \quad (3)$$

where γ is assumed to be 8.5° and the other notations are as given in Eqs. (1) and (2).

The experiment was performed before and the results were previously published by Kel *et al*. (2001), Copur *et al*. (2003) and Bilgin *et al*. (2006), they did the massive experiments on 11 different kinds of rock specimens on the full scale linear cutting machine. The entire experiment was carried out with an S-35/80 H conical pick manufactured by Sandvik. It has a gauge of 80 mm, flange diameter of 64 mm, shank diameter of 35 mm, tip diameter of 22 mm and primary tip angle of 80°. The constant conditions throughout the experiment are 55° of attack angle, 0° of skew and tilt angles. The depth of cut is changed from 3 to 10 mm. This paper references the results of unrelieved and relieved cutting modes to validate the reliability of numerical simulation.

3. THE GENERAL FORMULATION OF PFC^{3D}

PFC^{3D} is classified as a discrete element code based on the definition of the discrete element method proposed by Cundall and Hart (1992). It allows finite displacements and rotations of discrete bodies, including complete detachment, and recognizes new contacts automatically in the calculation progresses. The calculation cycle in PFC^{3D} is a time stepping algorithm that needs to apply the law of motion to each particle and a force-displacement law to each contact repeatedly, and constantly update the wall positions. A general view of ball-ball contact and ball-wall contact are shown in Fig. 3.

Whenever two particles overlap, a contact is formed at the center of the overlap region along the line joining the particle centers ($x_i^{[C]}$ in Fig. 3), and two linear springs are inserted along with a slider in the shear direction. The force-displacement law is

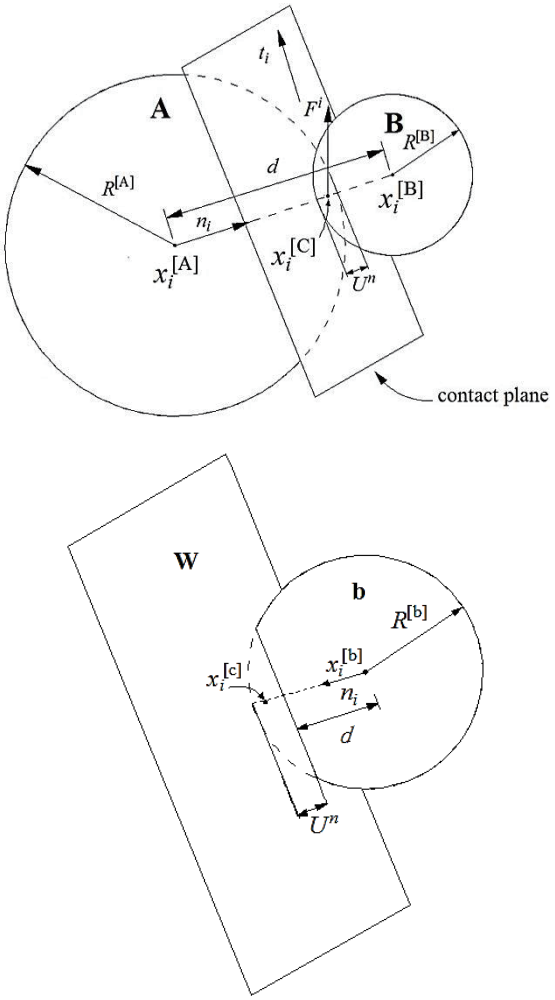

Fig. 3 Notation used to describe ball-ball contact and ball-wall contact (Itasca Consulting Group 2006)

described for both ball-ball and ball-wall contacts, and then the law is used to calculate the unbalanced forces on individual particle. The motion of particles and walls were tracked through the pointer (a data type, used for scanning through linked lists). The contact force vector F_i can be decomposed into normal and shear components with respect to the contact plane. Thereinto, the shear component is computed in an incremental mode. When the contact is formed, F_i^s is initialized to zero. Each subsequent relative shear-displacement increment ΔU_i^s produces an increment of elastic shear force ΔF_i^s, that is added to F_i^s. The calculation formulas are as follows (Potyondy and Cundall 2004; Itasca Consulting Group 2006; Iliescu *et al*. 2011):

$$F_i = F_i^n n_i + F_i^s t_i \quad (4)$$

$$F_i^n = K^n U^n \quad (5)$$

$$\Delta F_i^s = -k^s \Delta U_i^s \quad (6)$$

where F_i is the contact force, F_i^n and F_i^s denote the normal and shear force components, K^n is the contact normal stiffness,

U^n is the overlap, n_i and t_i are the unit normal and shear vectors, ΔF_i^s is the increment of elastic shear force, k^s is the shear stiffness and ΔU_i^s is the relative shear-displacement increment.

The motion of particles including movement and rotation depends on the force and torque acting on it. The equations of motion, given by Eqs. (7) and (8), are integrated using a centered finite difference procedure involving a timestep of Δt. The quantities $\dot{x}_i$ and $\dot{w}_i$ are computed at the mid-intervals of $t \pm n\Delta t/2$, while the quantities x_i, $\ddot{x}_i$, $\dot{w}_i$, F_i, and M_i are computed at the primary intervals of $t \pm n\Delta t$. The expression of vector formula is as follows (Itasca Consulting Group 2006)：

$$F_i = m(\ddot{x}_i - g_i) \quad \text{(translational motion)} \tag{7}$$

$$M_i = I\dot{w}_i = \left(\frac{2}{5}mR^2\right)\dot{w}_i \quad \text{(rotational motion)} \tag{8}$$

where F_i is the resultant force, the sum of all externally applied forces acting on the particle; m is the total mass of the particle; and g_i is the body force acceleration vector (*e.g.*, gravity loading). M_i is the resultant moment acting on the particle, I is the moment of inertia, R is the radius of spherical particle, w is the angular velocity.

4. NUMERICAL SIMULATION OF ROCK CUTTING

4.1 Calibration of the Model

Bilgin *et al*. (2006) did a lot of tests on the physical and mechanical properties of rock, such as uniaxial compressive strength, Brazilian tensile strength, static elasticity modulus *et al*. The mechanical parameters of rocks are shown in Table 1. It is necessary to calibrate the macro-properties of particle assemblies by simulating a lot of the uniaxial compressive strength and Brazilian tests before generating the rock specimens. The model of cylinder has the same size as the one measured in laboratory since the size effect has a great influence on the compressive strength, *i.e.*, diameter is 54 mm, and a length-to-diameter ratio 2.

The micro-parameters of particle assembly including particle parameters (namely density, radius ratio, Young's modulus, ratio of normal to shear stiffness and friction coefficient) and parallel bonding parameters (namely radius multiplier, Young's modulus, ratio of normal to shear stiffness, tensile strength and shear strength). Since these parameters could not be directly selected from the results obtained in laboratory, we had to adjust them by trial-and-error until the uniaxial compressive strength, elastic modulus and Poisson's ratio match with the measured values finally. In order to ensure that the pick contacted with the particle assembly at least four particles, the particle radius was set between 0.7 and 1.162 mm, and k_n / k_s and $\bar{k}_n / \bar{k}_s$ were taken the same value to reduce the number of free parameters. The macro-properties and the corresponding micro-properties after calibration are shown in Tables 2 and 3.

The macro-properties of four types of rocks were obtained from laboratory tests in Table 1, and those obtained from PFC^{3D} models in Table 2 were compared. The uniaxial compressive strength, Young's modulus and Poisson's ratio of the PFC^{3D} models agreed well with the experimental value while the other macro-properties deviated more. The Brazilian tensile strength was an average of five times larger than the value that measured in a valid Brazilian test. It is rather related to the particles size since the variability of tensile strength is much greater than that of compressive strength. In order to approach the measured value, the particles will have to be much smaller and this would make computations more time-consuming. Therefore, in this study, it is assumed that the uniaxial compressive strength test was sufficient to calibrate the specimen due to the uniaxial compressive strength was used to define the strength of rocks.

Table 1 Mechanical characteristics of rocks

Property	Medium-grade chromite	Sandstone-1	Sandstone-2	Sandstone-3
ρ (kg/m^3)	3390	2650	2670	2670
σ_c (MPa)	47	114	174	87
E (GPa)	2.3	17	28	33.3
v	0.2	0.2	0.29	0.25
σ_t (MPa)	4.5	6.6	11.6	8.3

Table 2 Macro-properties of rocks after calibration

Property	Medium-grade chromite	Sandstone-1	Sandstone-2	Sandstone-3
σ_c (MPa)	47.4	114.5	174.3	87.5
E (GPa)	2.4	16.8	27.2	34
v	0.23	0.24	0.3	0.26
σ_t (MPa)	24	51.4	61.68	21

Table 3 Model micro-properties for rocks

Rock types		Medium-grade chromite	Sandstone-1	Sandstone-2	Sandstone-3
Grain property	ρ (kg/m^3)	3390	2650	2670	2670
	R_{max}/R_{min}	1.66	1.66	1.66	1.66
	E_c (GPa)	5	34	50	65
	k_n / k_s	2	1.7	1.5	1.5
	μ	0.5	0.5	0.5	0.5
Cement property	$\bar{\lambda}$	1	1	1	1
	$\bar{E}_c$ (GPa)	5	34	50	65
	$\bar{k}_n / \bar{k}_s$	2	1.7	1.5	1.5
	$\bar{\sigma}_c$ (MPa)	138	365	518	237
	$\bar{\tau}_c$ (MPa)	138	365	518	237

ρ = density, R_{max}/R_{min} = radius ratio, E_c = Young's modulus, k_n / k_s = ratio of normal to shear stiffness for grain properties, μ = friction coefficient, $\bar{\lambda}$ = radius multiplier, $\bar{E}_c$ = Young's modulus, $\bar{k}_n / \bar{k}_s$ = ratio of normal to shear stiffness for parallel bond properties, $\bar{\sigma}_c$ = tensile strength, $\bar{\tau}_c$ = shear strength.

4.2 Modeling of Rock Cutting

After calibration, the rectangular parallelepiped specimens were generated by the specimen-genesis procedures proposed by Potyondy and Cundall (2004), with dimension of 70 × 90 × 42 mm^3, containing approximately 50882 particles. Two conical picks with rounded tip were positioned through the left side of the specimen at the optimum *s*/*d* ratio, and the attack angle is 55°, tip angle is 80°, the depth of cut is 9 mm, those parameters consistent with the test conditions, as is shown in Fig. 4.

At the beginning of the simulation, top and lateral walls of the specimen were deleted and the particles which are close to the bottom wall were fixed. The quasi-static equilibrium is determined based on an equilibrium ratio limit, it expressed as the ratio of maximum unbalanced force magnitude divided by average unbalanced force magnitude over all particles. When particle assembly was squeezed by walls at a constant velocity, that could cause the internal unbalanced force increases rapidly and the initial equilibrium state was destroyed. While the internal stress state of particle assembly has a very large impact on the forces suffered by walls. Assuming that the equilibrium ratio limit is 1×10^{-3} in this study, some tentative simulations were carried out by using different cutting velocities. After comprehensive considering the program running time and the defined equilibrium ratio limit, the cutting velocity of 0.25 m/s was selected in this simulation. The cutting distance of 30 mm was applied to ensure that the simulation of rock cutting process kept a long-term stable cutting state within a range of acceptable calculation time. Firstly, $1^{\#}$ pick was participated in the rock cutting until the cutting distance reach to set value, then the walls comprise $1^{\#}$ pick were deleted, $2^{\#}$ pick has begun to contact with the particle assembly, and be involved in relieved cutting, the cutting distance was the same to the first cut.

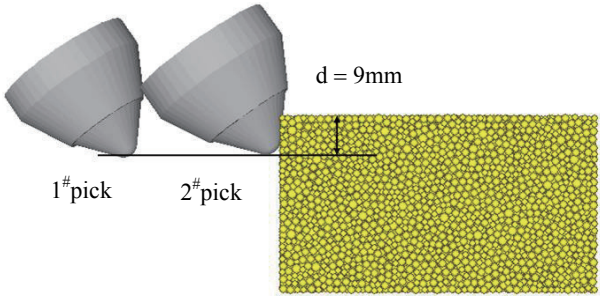

(a) Front view

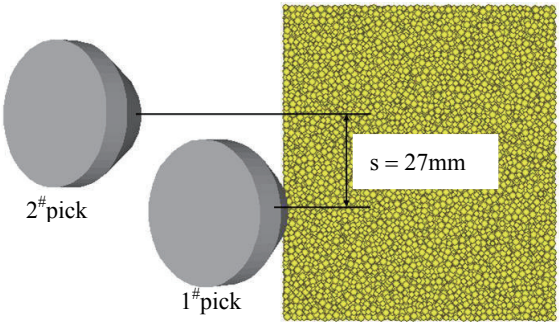

(b) Top view

Fig. 4 The model of rock cutting

In the simulation of rock cutting process, the pick forces are decomposed into three orthogonal forces: Normal, cutting and sideway forces. Cutting force is applied in line with the cutting direction, normal force act on perpendicular to the direction of cutting, and sideway force is also measured transverse to the direction of cutting. The cutting, normal and sideway forces acting on pick were monitored in the numerical simulation, and the bond breakages between particles in both the normal and tangential directions were recorded. According to the simulation data, the mean forces in three directions were estimated, and the mean peak cutting forces were calculated, which accepted as the average of maximum forces in twenty increments of force data. When the pick began to interact with particles, the bonding failure would occur, and micro-cracks were come into being. With the number of fractures increased, micro-cracks were gradually propagated from the pick tip which led to chips formed. The sandstone-3 specimen suffered the destruction at the depth of cut of 9 mm in unrelieved and relieved cutting modes, as shown in Fig. 5, and the corresponding left side view and top view were described in Fig. 6. The red and black cylinders represented the fractures formed in normal and shear failure during the cutting process, and there was formed a ridge between the first and second cuts after the simulation of rock cutting was finished.

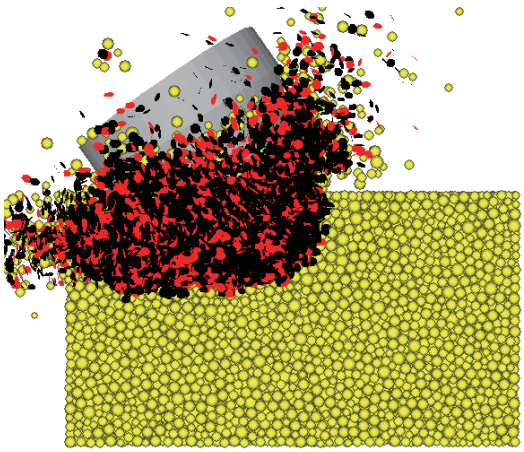

Fig. 5 Micro-cracks occurring around $1^{\#}$ pick at the depth of cut of 9 mm

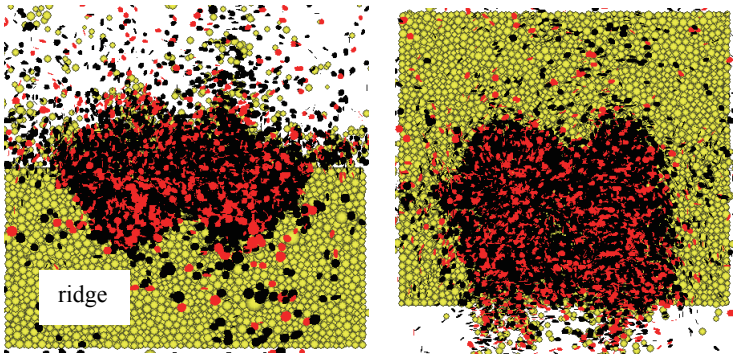

Fig. 6 Left side view and top view of destructed specimen with two picks

5. RESULTS, VALIDATION AND DISCUSSIONS

In this context, the macro-properties such as uniaxial compressive strength, Young's modulus and Poisson's ratio of specimens were calibrated by recurring those measured from laboratory in PFC^{3D}. The micro-parameters obtained by calibration were input into the specimen-genesis procedure and generate the rectangular parallelepiped particle assemblies. The normal, cutting and sideway forces were recorded, and corresponding force-distance curves were redrew by using MATLAB.

The variations of forces with cutting distance in three directions of sandstone-3 at the optimum conditions (s/d ratio is 3; the depth of cut is 9 mm) were described in Figs. 7, 8, and 9. The force-distance curves of 1$^{\#}$ and 2$^{\#}$ picks were plotted by lines with black and red colors respectively. Obviously, the mean cutting and normal forces obtained in relieved cutting mode are lower than those in unrelieved mode in Figs. 7 and 9. It was pointed out that the interaction of two picks made the forces in normal and tangential directions decreased in relieved cutting mode. The sideway force was fluctuated up and down in the vicinity of x-axis and corresponding mean value was close to zero in unrelieved cutting mode, but a negative mean value below the x-axis was obtained in relieved cutting mode, as is shown in Fig. 8.

When the particle assembly was squeezed by walls (pick) continuously, all subsequent bond breakages will be tracked as cracks. The variations of the number of cracks with cutting distance in tensile and shear failure modes were described in Fig. 10. It is known that the tensile failure mode was assumed in Evans' model. Seen from Fig. 10, the number of cracks in tensile failure is three times larger than those in shear failure, thus the fractures mainly in tensile failure was verified by theoretical model. In addition, regression analysis was performed to analyze the variation of bond breakages at the first and second cuts in both failure modes, the mathematic models of simple linear regression were established, these equations showed that the increment speed of bond breakages at the second cut is evidently less than that at the first cut.

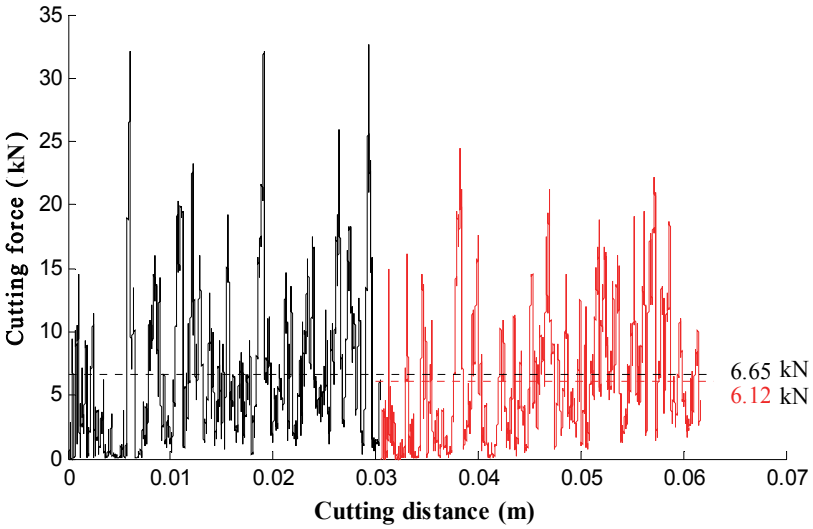

Fig. 7 The variation of cutting force versus cutting distance

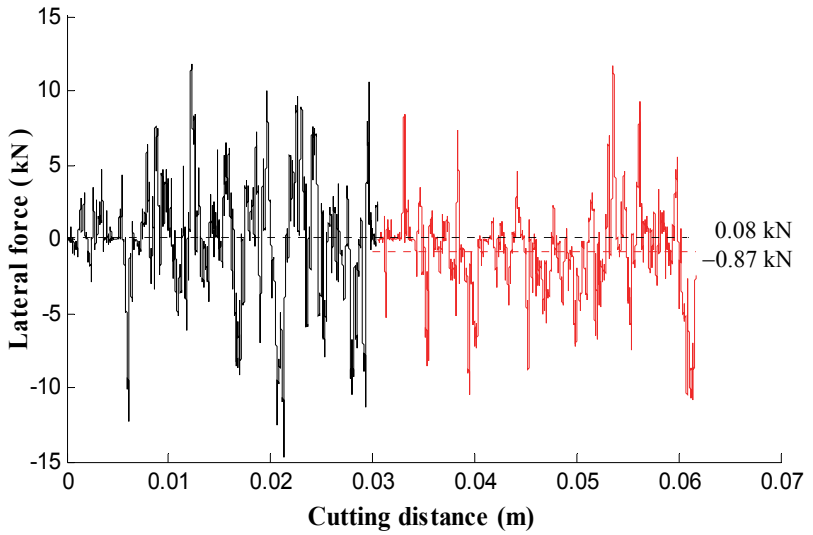

Fig. 8 The variation of lateral force versus cutting distance

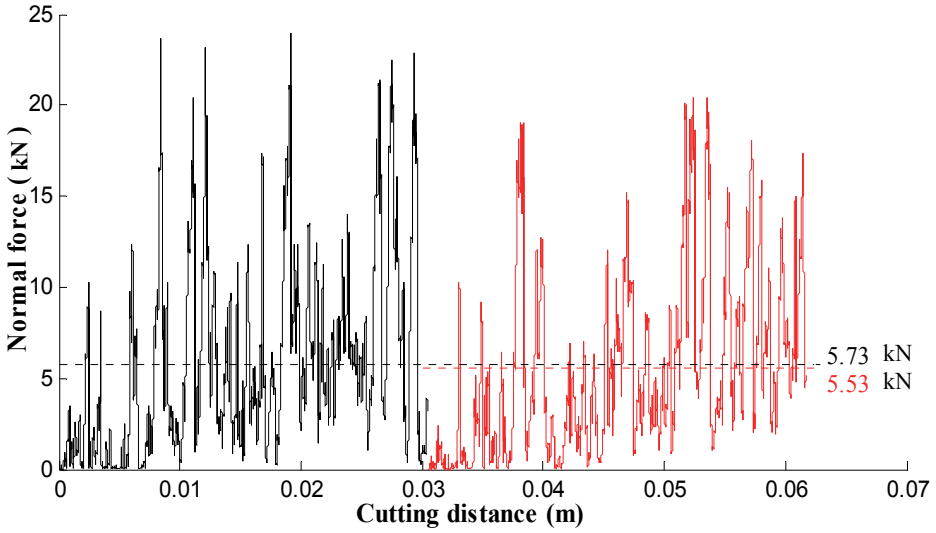

Fig. 9 The variation of normal force versus cutting distance

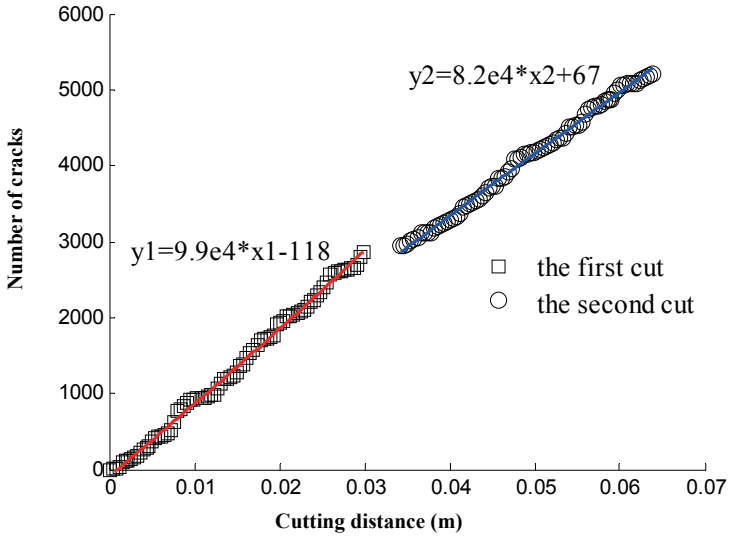

(a) Tensile failure

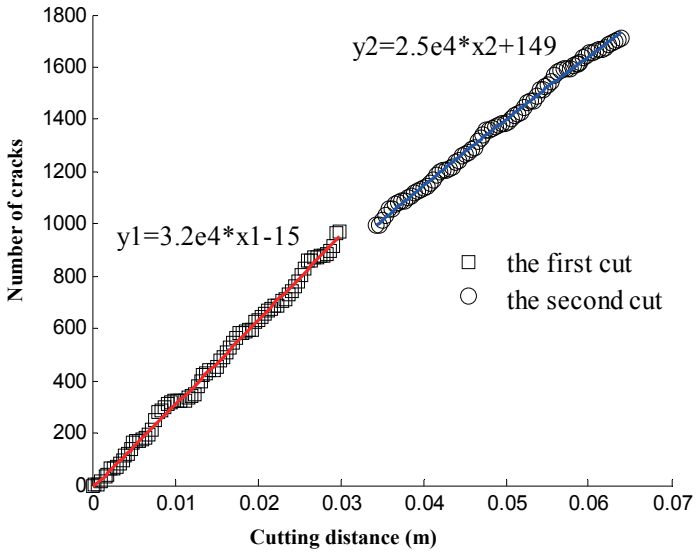

(b) Shear failure

Fig. 10 The variation of the number of cracks with cutting distance

From Table 4, there is a small gap between numerical and experimental studies about the mean forces and mean peak forces in unrelieved cutting mode. Compared with the experimental results, the forces predicted by theoretical formulas are significantly lower. An important conclusion can be drawn that the numerical simulation model can be predict the mean peak cutting force reliably, but these formulas can not. Since there exist many uncertain factors during the tests in laboratory, such as temperature, wear, *etc.,* and the particle assembly has the characteristic of isotropy and homogeneousness in PFC^{3D}. Therefore, the difference between test and simulation is expected.

In relieved cutting mode, the results of forces obtained from numerical and experimental studies are shown in Table 5. It can be seen that the numerical studies are a bit higher than experimental studies in terms of the mean forces and maximum forces.

In practical engineering, the ratio of peak to mean forces is an important factor affecting on cutterhead vibration, which can cause the mechanical parts failure. In Table 6, simulation results agree well with the experimental results, and we can found that the ratio of peak to mean forces was affected by rock properties slightly, which is in accordance to the findings of Bilgin *et al.* (2006). The ratio of peak to mean cutting forces and the ratio of peak to mean normal forces are 2.68 ± 0.4SD (standard deviation) and 3.06 ± 0.49SD for unrelieved cutting mode and 3.11 ± 0.44SD and 3.07 ± 0.32SD for relieved cutting mode respectively. It was seen that the values obtained in relieved cutting were higher than those in unrelieved cutting, since the larger chips were generated in relieved cutting and that could cause the peak forces increased.

Table 4 The results of forces obtained from numerical, theoretical and experimental studies in unrelieved cutting mode

Rock type	Cutting force of numerical simulation (kN)				Theoretical cutting force (kN)			Experiment cutting force (kN)			
	F_C	F_N	F_C'	F_N'	$F_{C\,\mathrm{Evans}}'$	$F_{C\,\mathrm{Goktan}}'$	$F_{C\,\mathrm{Rox}}'$	F_C	F_N	F_C'	F_N'
Sandstone-1	13.58	14.32	28.55	29.85	2.65	5.68	4.11	9.72	8.52	28.93	21.45
Sandstone-2	22.43	21.34	42.28	43.19	5.36	10	7.86	16.52	18.9	47.14	42
Sandstone-3	6.65	5.73	15.85	13.24	5.49	7.86	6.76	6.42	5.9	15.6	12.7
Medium-grade chromite	11.31	12.37	17.85	18.77	3	3.88	3.67	9.12	6.53	25.96	16.16

F_C = mean cutting force, F_C' = mean peak cutting force, F_N = mean normal force, F_N' = mean peak normal force

Table 5 The results of forces obtained from numerical and experimental studies at optimum ratio (*s*/*d*) in relieved cutting mode

Rock type	Cutting force of numerical simulation (kN)				Experiment cutting force (kN)				Optimum (*s*/*d*) ratio
	F_C	F_N	F_C''	F_N''	F_C	F_N	F_C''	F_N''	
Sandstone-1	9.63	11.96	26.96	32.27	7.85	7.94	23.24	18.26	2
Sandstone-2	13.33	14.84	39.99	44.52	9.17	11.29	27.61	25.63	2
Sandstone-3	6.12	5.53	24.43	20.4	4.76	4.06	13.67	9.74	3
Medium-grade chromite	6.25	5.32	16.47	15.28	4.59	3.35	13.04	8.85	2

F_C = mean cutting force, F_C'' = maximum cutting force, F_N = mean normal force, F_N'' = maximum normal force

Table 6 The ratio of peak to mean force in numerical and experimental studies in both cutting modes

Cutting mode	Ratio of peak to mean forces in PFC^{3D}		Ratio of peak to mean forces in Lab	
	F_C''/F_C	F_N''/F_N	F_C''/F_C	F_N''/F_N
Unrelieved cutting	2.68 ± 0.4	3.06 ± 0.49	2.69 ± 0.32	2.39 ± 0.33
Relieved cutting	3.11 ± 0.44	3.07 ± 0.32	3.07 ± 0.55	2.64 ± 0.49

6. CONCLUSIONS

In this paper, the numerical modeling of the rock cutting test was carried out in unrelieved and relieved cutting modes, and the forces acting on pick were monitored. The mean peak cutting force were calculated by theoretical formulas in unrelieved cutting mode, and the experimental results in laboratory were also given.

In both cutting modes, there is a small gap between numerical and experimental studies about the mean forces and mean peak forces. Since there were many uncertain factors existed in the test, such as temperature, wear *etc.,* and the particle assembly has the characteristic of isotropy and homogeneousness, the difference between test and simulation is expected. Additionally, the numerical results agree well with the experimental results in terms of the ratio of peak to mean forces, and then the advantages of distinct element method in simulating the rock cutting test were validated.

The numerical force-distance curves of pick were compared between the unrelieved and relieved cutting mode. Affecting by the adjacent cut, it can be seen that the cutting and normal forces decreased and sideway force increased in relieved cutting mode.

The subsequent bond breakages were formed in the process of the particle assembly was squeezed by walls (pick), which will be tracked as cracks. The records showed that the number of cracks in tensile failure is about three times larger than those in shear failure, thus the formation of fractures was mainly in tensile failure mode. Moreover, regression analysis was applied to

analyze the variation of bond breakages in both cutting mode, the results indicated that the increment speed of bond breakages in relieved cutting mode is evidently less than those in unrelieved cutting mode.

ACKNOWLEDGMENTS

The research is supported by Basic Research Program of Shanxi Province, Grant No. 2015011061, Basic Research Program of Shanxi Province, Grant No. 2015021135, and National High Technology Research and Development Program of China, Grant No. 2012AA06A405.

REFERENCES

Bilgin, N., Demircin, M.A., Copur, H., Balci, C., Tuncdemir, H., and Akcin, N. (2006). "Dominant rock properties affecting the performance of conical picks and the comparison of some experimental and theoretical results." *International Journal of Rock Mechanics and Mining Sciences*, **43**, 139–156.

Copur, H., Bilgin, N., Tuncdemir, H., and Balci, C. (2003). "A set of indices based on indentation tests for assessment of rock cutting performance and rock properties." *Journal of the South African Institute of Mining and Metallurgy*, 589–599.

Cundall, P.A. and Hart, D.H. (1992). "Numerical modelling of discontinua." *Engineering Computation*, **9**, 101–113, DOI: 10.1108/eb023851.

Evans, I. (1984). "A theory of the cutting force for point-attack pick." *International Journal of Mining Engineering*, **2**, 63–71.

Gokan, R.M. (1997). "A suggested improvement on Evans' cutting theory for conical bits." *Proceedings of the Fourth symposium on Mine Mechanization Automation,* Brisbane, Queensland, 57–61.

Itasca Consulting Group (2006). *Particle Flow Code in 3 Dimensions Manual,* Version3.1, Minneapolis, Itasca.

Iliescu, D., Gehin, D., Iordanoff, I., Girot, F., and Gutiérrez, M.E. (2011). "A discrete element method for the simulation of CFRP cutting." *Composites Science and Technology*, **70**, 73–80.

Kel, K., Akçin, N., Tunçdemir, H., and Bilgin, N. (2001). "Cuttability characteristics of high strength rocks for roadheader selection in Zonguldak Coalfiled." *Proceedings of the 10th International Symposium on Mine Planning & Equipment Selection*, New Delhi, 789–795.

Moon, T. and Oh, J., (2012). "A study of optimal rock-cutting conditions for hard rock TBM using the discrete element method." *Rock Mechanics and Rock Engineering*, **45**, 837–849.

Potyondy, D.O. and Cundall, P.A. (2004). "A bonded-particle model for rock." *International Journal of Rock Mechanics and Mining Sciences*, **41**, 1329–1364.

Rojek, J. and Onate, E. (2011). "Discrete element simulation of rock cutting." *International Journal of Rock Mechanics and Mining Sciences*, **48**, 996–1010.

Roxborough, F.F. and Liu, Z.C. (1995). "Throretical considerations on pick shape in rock and coal cutting." *Proceedings of the Sixth Underground Operator's Conference*, Kalgoorlie, Australia, 189–193.

Su, O. and Akcin, N.A. (2008). "Modeling of unrelieved rock cutting test by using PFC^{3D}." *Proceedings of the First International FLAC/DEM Symposium*, Minneapolis, 165–172.

Su, O. and Akcin, N.A. (2009). "Numerical simulation of rock cuttability." *Proceedings of the International Conference on Rock Joints & Jointed Rock Masses*, Tucson, Ariz (CD).

Su, O. (2011). "Numerical simulation of rock cutting using the discrete element method." *International Journal of Rock Mechanics and Mining Sciences*, **48**, 434–442.

van Wyk, G., Els, D.N.J., Akdogan, G., Bradshaw, S.W., and Sacks, N. (2014). "Discrete element simulation of tribological interactions in rock cutting." *International Journal of Rock Mechanics and Mining Sciences*, **65**, 8–19.

Yong, L., Dekun, Z., Qingliang, W., Hongtao, L., Gang, C., and Shirong, G. (2010). "Preparation and properties of a new cutting pick of coal shearers." *International Journal of Mining Science and Technology*, **20**, 794–796.